Resilience Enhancement Strategy for Distribution Systems Under Extreme Weather Events

Shanshan Ma, *Student Member, IEEE*, Bokan Chen, *Student Member, IEEE*, and Zhaoyu Wang, *Member, IEEE*

***Abstract*—This paper proposes an optimal hardening strategy to enhance the resilience of power distribution networks to protect against extreme weather events. Different grid hardening techniques are considered, such as upgrading poles and vegetation management. The problem is formulated as a tri-level optimization problem to minimize grid hardening investment and load shedding in extreme weather events. The first level is to identify vulnerable distribution lines and select hardening strategies, the second level is to determine the set of out-of-service distribution lines so that the damage caused by extreme weather events is maximized, and the third level is to minimize load shedding costs according to load priorities and the set of damaged lines. Since the selection of hardening strategies is coupled with the uncertainty set of out-of-service lines, the original tri-level model is transformed to be an equivalent bi-level problem, which is subsequently solved by a greedy searching algorithm. Case studies demonstrate the effectiveness of the proposed method under multiple severe weather events and different simulation settings.**

***Index Terms*—Distribution systems, failure probability, extreme weather events, power system resilience.**

NOMENCLATURE

Sets and Indices

Ω_N	Set of nodes
Ω_B	Set of lines
Ω_x	Set of hardening strategies
Ω_G	Set of distributed generators (DGs)
Ω_L	Set of loads
$\mathcal{T}$	Set of durations of extreme weather events
χ	Set of system hardening decisions
$\mathcal{U}$	Uncertainty set of extreme weather events
$\mathcal{O}$	System operation set under extreme weather events
i	Node index
(i, j)	Line index
k	Hardening strategy index
t	Time index.

Parameters

B_L	Hardening investment budget
c_{ij}^k	Cost of kth hardening strategy at line ij
c_i^L	Cost of shedding ith load
T_R	Repair time
$\mathcal{W}$	Uncertainty Budget
$P_{i,t}^L/Q_{i,t}^L$	Active/Reactive load demand
$P_{i,t}^{g,\max}/Q_{i,t}^{g,\max}$	Active/Reactive power limits of DG
$P_{ij}^{\max}/Q_{ij}^{\max}$	Active/Reactive power limit of line ij
R_{ij}/X_{ij}	Resistance/Reactance of line ij
$\lvert V_i\rvert^{\max}/\lvert V_i\rvert^{\min}$	Maximum/Minimum voltage magnitude
V_0	Reference voltage magnitude
M_1/M_2	Big numbers.

Variables

$p_{ij,t}^k$	Failure probability of line ij after implementing kth hardening strategy
x_{ij}^k	Binary variable indicates whether kth hardening strategy is selected (1) or not (0) at line ij
$z_{ij,t}^k$	Binary variable indicates whether the line ij (after being hardened by the kth hardening strategy) is failed (1) or not (0) at time t
$u_{ij,t}$	Binary variable indicates the actual damage state of line ij at time t: damaged (1) or not (0)
$\rho_{i,t}$	Load shedding ratio
$P_{ij,t}/Q_{ij,t}$	Active/Reactive power flow
$P_{i,t}^g/Q_{i,t}^g$	Active/Reactive power output of DGs
$\lambda_{i,t}^k, \lambda_{ij,t}^k$	Dual variables.

Manuscript received February 5, 2016; revised May 14, 2016; accepted July 4, 2016. Date of publication July 18, 2016; date of current version February 16, 2018. This work was supported by the Electric Power Research Center at Iowa State University. Paper no. TSG-00177-2016.

S. Ma and Z. Wang are with the Department of Electrical and Computer Engineering, Iowa State University, Ames, IA 50014 USA (e-mail: sma@iastate.edu; wzy@iastate.edu).

B. Chen is with the Department of Industrial and Manufacturing Systems Engineering, Iowa State University, Ames, IA 50014 USA (e-mail: bokanc@iastate.edu).

Color versions of one or more of the figures in this paper are available online at http://ieeexplore.ieee.org.

Digital Object Identifier 10.1109/TSG.2016.2591885

I. INTRODUCTION

ENHANCING grid resilience to protect against extreme weather events is a key task of grid modernization efforts [1]. The extreme weather-caused outages have resulted in substantial economic losses in recent years in the United States. For example, Hurricane Sandy in 2012 paralyzed power systems of several coastal states and resulted in outages that affected over 8.5 million customers [2]. It is reported that 65% of New Jersey's customers were disconnected from grids in this severe event [3]. Between 2003 and 2012, roughly 679 power outages, each affecting at least 50, 000 customers, occurred due to weather events in the United States, and 80%−90% of these outages were due to failures in distribution systems [4].

Grid hardening is one of the most effective methods to protect systems against extreme weather events. There are various grid hardening strategies such as overhead structure reinforcement, vegetation management, undergrounding, and integrating black-start resources. Overhead structure reinforcement constitutes a primary hardening strategy which involves upgrading distribution poles to a stronger class, enhancing guying, and refurbishing poles. Extensive vegetation management can also contribute to distribution system hardening, as fallen trees and debris are credited with the majority of power outages that occur during severe storms in the Northeastern part of the United States [5]. Undergrounding distribution lines can reduce the system's susceptibility to wind-induced damages, lightning, and vegetation contacts, but it extends the restoration time with a high installation and repair cost. Elevating substations, integration of DGs, and relocating facilities to areas that are less prone to extreme weather can help protect against floods. Although system hardening could reduce component failures and restoration efforts, hardening and upgrading the entire distribution systems is potentially expensive. As a result, how to cost-effectively design a resilient distribution system against climatic disasters becomes a great challenge.

Based on previous hurricanes' impacts on power systems, there are two major questions on distribution system hardening [6]. One is how to prioritize distribution lines for hardening, and the other is what hardening efforts should be performed on each line. A commonly used way of implementing mitigation strategies is to upgrade previously damaged facilities or perform targeted hardening based on experiences. Over the years, several methods of hardening distribution systems have been studied with the objective to improve the system reliability, such as risk-analysis and optimization techniques. In [2], authors propose a targeted hardening strategy to improve distribution system reliability, which involves strengthening important distribution poles as well as poles with a high probability of failure by identifying risk-critical parts of the system. In [7], a vegetation management scheduling algorithm that determines the optimal location and time to perform vegetation maintenance on overhead distribution lines is presented. However, these two papers are limited to certain types of weather events and single hardening techniques. The uncertain traveling paths and severities of extreme weather events, and their impacts on system resilience are neglected.

A few optimization models are proposed to facilitate the grid hardening decision-making process and most of them focus on transmission networks [3], [8], [9]. The optimal hardening problem is generally formulated as a bi-level or tri-level problem. For a bi-level formulation, the upper level selects hardening strategies with the objective of minimizing investment, and the lower level evaluates the benefits of hardening using a set of sampled damage scenarios [3]. In a tri-level formulation, a defender-attacker-defender model is generally applied [8], [9]. The system planner identifies the components to be hardened in the upper level. In the middle level, the disruption model determines the set of out-of-service components so that the damage in the system is maximized. In the lower level, the system operator minimizes the damage using optimal operation strategies. However, the diversity and time-varying uncertainty of extreme weather events are not taken into account in these methods. Furthermore the hardened components are assumed to have a zero failure rate which is impractical.

A distribution system is considered to be resilient if it is able to anticipate, absorb, adapt to, and/or rapidly recover from a disruptive event [10]. This paper proposes an optimal hardening strategy to enhance the resilience of distribution networks. The objective is to take optimal pre-event resilience-enhancement actions to reduce the failure probability of distribution systems and mitigate consequences of these failures. A tri-level optimization model that considers the failure probability of hardened components is formulated. Compared to methods in [2] and [7] which only consider a single hardening strategy, there are three different hardening strategies for each line to select according to hardening costs and weather parameters in this paper. We propose a new infrastructure fragility model to represent the spatial-temporal impacts of extreme weather events on the resilience of distributed lines that have been hardened. The model is then incorporated in the time-varying uncertainty set of the tri-level optimization model to evaluate the system resilience. A new solution methodology is proposed to solve the tri-level problem with coupled variables in its first and second levels. The tri-level program is transformed into an equivalent bi-level mixed-integer linear program by reformulating the max-min structure in its second and third levels into a single-level equivalent. An effective greedy algorithm is presented to solve the resulted bi-level optimization problem by finding critical lines firstly and then hardening these lines with the minimum investment.

The rest of the paper is organized as follows. Section II provides fragility models and resilience enhancement strategies. Section III proposes mathematical formulations. Section IV reformulates the problem into a bi-level problem and develops a new solution algorithm. Numerical results are presented in Section V. Section VI concludes the paper.

II. Infrastructure Fragility Models and Resilience Enhancement Strategies

This section introduces the proposed infrastructure fragility model for power distribution systems with both overhead and underground systems and three resilience-enhancement strategies. The fragility analysis calculates the time-varying failure probability of hardened distribution lines considering wind speed's impacts on distribution poles and tree contacts, and floods' impact on underground systems. The fragility model of distribution lines is used to set the time-varying uncertainty set of extreme weather events in the tri-level hardening optimization model.

A. Fragility Models of Overhead Systems

For overhead systems, the majority of power outages happen because trees are blown into power lines, and/or high intense winds directly blow down poles during hurricanes,

wind storms and winter storms [11]. Overhead distribution lines consist of poles, conductor wires and other types of equipment [12]. The breakdown of a single pole or conductor results in the disconnection of the entire line. Hence, the fragility of a distribution line can be modeled as a series system with the fragility analysis of each pole and conductor within that line [12]. It is assumed that the fragility of different components of an overhead line is independent. The failure probability of an overhead line before being damaged by extreme weather events can be expressed as follows:

$$p_{l,ij}(v(t)) = 1 - \prod_{k=1}^{m} \left(1 - p_{I_k}(v(t))\right) \prod_{k=1}^{n} \left(1 - p_{fc,k}(v(t))\right) \quad (1)$$

where $p_{l,ij}(v(t))$ is the failure probability of the overhead line ij; m is the number of distribution poles supporting line ij; n is the number of conductor wires between two adjacent poles at line ij. p_{I_k} is defined as the conditional probability of kth poles at line ij as a function of the wind speed, and it can be modeled as a lognormal cumulative distribution function (CDF) [2]:

$$p_{I_k}(v(t)) = \Phi\left[\ln\left((v(t)/m_R)/\xi_R\right]\right. \quad (2)$$

where $v(t)$ is the local 3-s gust wind speed, m_R is the median capacity or resistance, and ξ_R is the logarithmic standard deviation of intensity measurement.

$p_{fc,k}(v(t))$ represents the failure probability of conductor k between two poles:

$$p_{fc,k}(v(t)) = (1 - \mathrm{f}_u) \max\left(p_{fw,k}(v(t)), \alpha p_{ftr,k}((v(t)))\right. \quad (3)$$

where $p_{fw,k}(v(t))$ represents the direct wind-induced failure probability of conductor k; $p_{ftr,k}$ represents the fallen tree-induced failure probability of conductor k; f_u represents the probability that conductor k is undergrounded (invulnerable to extreme weather events), and is set as 0.32; and α represents the average tree-induced damage probability of overhead conductors. The direct wind-induced damage probability of the conductor k can be model by [12]:

$$p_{fw,k}(v(t)) = \min\left\{F_{fw,k}(v(t))/F_{fo,k}(v(t)), 1\right\} \quad (4)$$

where $F_{fw,k}(v(t))$ represents the wind force on conductor k; and $F_{fo,k}(v(t))$ represents the maximum perpendicular force that conductor k can endure.

$p_{ftr,k}(v(t))$ can be represented as follows [13]:

$$p_{ftr,k}((v(t)) = \frac{e^{h(S_k)}}{1 + e^{h(S_k)}} \quad (5)$$

$$h(S_k) = a_s + c_s(k_s S_k) D_H^{b_s} \quad (6)$$

where S_k is the wind intensity ($0 - 1$ scale) at conductor k, and can be calculated by dividing the local $3 - s$ wind speed by the maximum wind speed in the studied area [13]; D_H is the tree diameter at its breast height (1.35m); k_s is a factor to consider local terrain effects, and is chosen based on the land cover information near conductor k; a_s, b_s and c_s are parameters related with tree species.

TABLE I
RESILIENCE ENHANCEMENT STRATEGIES FOR DISTRIBUTION LINES

No.	Strategies	Primary Lines	Large Laterals
1	Upgrading distribution poles	\$5,924/pole	\$5,000/pole
2	Vegetation management	\$20,095/mile	\$39,936/mile
3	Combination of 1 and 2*	\$227,435/mile	\$214,936/mile

*Assume the span of two consecutive poles is 150 ft.

B. Flood-Induced Failures in Underground Systems

A storm surge is a wall of water that floods the shore and the adjacent land as a hurricane approaches the land [14]. When a storm surge recedes from the land, underground wires and other components are damaged due to water exposure, debris and salt residual [14]. Currently, the data on storm surges is insufficient to determine the best mathematical model for flood or storm surge-induced damages. However, the following linear function can be used to estimate underground system damages based on categories of hurricanes and storm surge zones [14].

$$p_{ung,ij,t} = [a + b(H - S_z)] \cdot I(H - S_z) \quad (7)$$

$$I(H - S_z) = \begin{cases} 1 & H - S_z \geq 0 \\ 0 & H - S_z < 0 \end{cases} \quad (8)$$

where $p_{ung,ij,t}$ is the failure probability of underground line ij, H is the hurricane category, S_z is the storm surge zone category, and a and b are tuning parameters. Equation (8) is an indicator function which shows whether the area is affected by an incoming hurricane.

C. Resilience Enhancement Strategies

Based on the above fragility analysis of distribution lines, we consider three resilience-enhancement strategies as shown in Table I [15]. Strategy 1 is to replace a pole with a higher-class one. Strategy 2 is to trim trees to make their diameters at breast heights less than 10 cm [13]. Strategy 3 is the combination of strategy 1 and strategy 2. In addition, it is assumed that Strategy 4 represents no hardening is implemented.

III. MATHEMATICAL FORMULATIONS

We propose a tri-level model as shown in Fig. 1. The objective is to minimize the hardening investment and the load shedding under the worst case scenarios. The first level is to identify hardening strategies. In the second level, the uncertainty set of failed lines is determined based on the severity of extreme weather events so that the damage of distribution systems is maximized. The third level is to minimize the cost of load shedding due to the physical damage of distribution lines in the second level.

The proposed formulation is introduced as follows:

$$\min_{x \in \chi} \left\{ \mathcal{C}^I(x) + \max_{u \in \mathcal{U}(x)} \min_{o \in \mathcal{O}(u)} \mathcal{C}^S(o) \right\} \quad (9)$$

subject to:

$$\mathcal{C}^I(x) = \sum_{k,ij} c_{ij}^k x_{ij}^k, \forall (i,j) \in \Omega_B, k \in \Omega_x, t \in \mathcal{T} \quad (10)$$

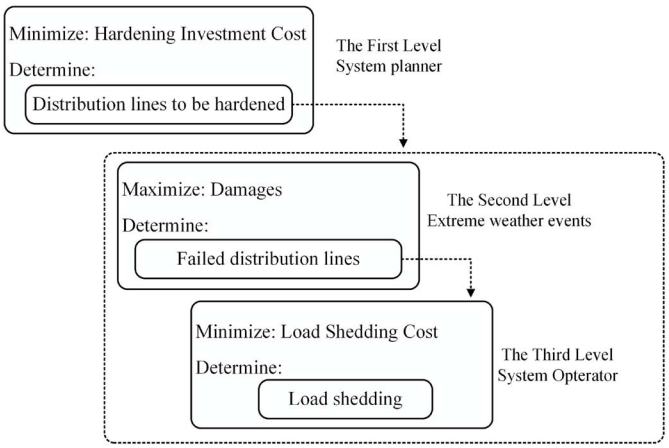

Fig. 1. The proposed tri-level model for power distribution system hardening.

$$\mathcal{C}^S(o) = \sum_{i,t} c_i^L \rho_{i,t} P_{i,t}^L, \forall i \in \Omega_L, t \in \mathcal{T} \tag{11}$$

$$\mathcal{C}^I(x) \le B_L \tag{12}$$

$$\chi = \left\{ x \left| \sum_{k \in \Omega_x} x_{ij}^k = 1, \forall k \in \Omega_x, (i,j) \in \Omega_B, x_{ij}^k \in \{0,1\} \right. \right\} \tag{13}$$

$$\mathcal{U} = \left\{ \mathbf{u} \left| \sum_{(i,j) \in \Omega_B} \left(-\log_2 p_{ij,t}^k \right) z_{ij,t}^k \le \mathcal{W}, \quad \forall k \in \Omega_x, t \in \mathcal{T} \right. \right. \tag{14}$$

$$z_{ij,t}^k \le x_{ij}^k, \forall k \in \Omega_x, (i,j) \in \Omega_B, t \in \mathcal{T} \tag{15}$$

$$\sum_t z_{ij,t}^k \le 1, \forall k \in \Omega_x, (i,j) \in \Omega_B, t \in \mathcal{T} \tag{16}$$

$$u_{ij,t} \le \sum_{st=t-T_R}^{t} z_{ij,st}^k, \forall k \in \Omega_x, (i,j) \in \Omega_B, t \in \mathcal{T} \tag{17}$$

$$\left. u_{ij,t}, z_{ij,t}^k \in \{0,1\}, \forall k \in \Omega_x, (i,j) \in \Omega_B, t \in \mathcal{T} \right\} \tag{18}$$

$$\mathcal{O}(u) = \left\{ o \left| \sum_{\{j|(i,j) \in \Omega_B\}} P_{ij,t} = \sum_{\{j|(i,j) \in \Omega_B\}} P_{ji,t} - P_{i,t}^g \right. \right.$$
$$- \left(1 - \rho_{i,t}\right) P_{i,t}^L, \forall i \in \Omega_N, t \in \mathcal{T} \quad \left[\lambda_{i,t}^1\right] \tag{19}$$

$$\sum_{\{j|(i,j) \in \Omega_B\}} Q_{ij,t} = \sum_{\{j|(i,j) \in \Omega_B\}} Q_{ji,t} - Q_{i,t}^g - \left(1 - \rho_{i,t}\right) Q_{i,t}^L,$$
$$\forall i \in \Omega_N, t \in \mathcal{T} \quad \left[\lambda_{i,t}^2\right] \tag{20}$$

$$0 \le P_{ij,t} \le \left(1 - u_{ij,t}\right) P_{ij}^{\max},$$
$$\forall (i,j) \in \Omega_B, t \in \mathcal{T} \quad \left[\lambda_{ij,t}^3\right] \tag{21}$$

$$0 \le Q_{ij,t} \le \left(1 - u_{ij,t}\right) Q_{ij}^{\max},$$
$$\forall (i,j) \in \Omega_B, t \in \mathcal{T} \quad \left[\lambda_{ij,t}^4\right] \tag{22}$$

$$\left|V_{j,t}\right| \le \left|V_{i,t}\right| - \frac{R_{ij} P_{ij,t} + X_{ij} Q_{ij,t}}{V_0} + u_{ij,t} M_1$$
$$\forall i \in \Omega_N, t \in \mathcal{T} \quad \left[\lambda_{i,t}^5\right] \tag{23}$$

$$\left|V_{i,t}\right| - \frac{R_{ij} P_{ij,t} + X_{ij} Q_{ij,t}}{V_0} - u_{ij,t} M_1 \le \left|V_{j,t}\right|$$
$$\forall i \in \Omega_N, t \in \mathcal{T} \quad \left[\lambda_{i,t}^6\right] \tag{24}$$

$$0 \le P_{i,t}^g \le P_{i,t}^{g,\max}, \quad \forall i \in \Omega_G, t \in \mathcal{T} \quad \left[\lambda_{i,t}^7\right] \tag{25}$$

$$0 \le Q_{i,t}^g \le Q_{i,t}^{g,\max}, \quad \forall i \in \Omega_G, t \in \mathcal{T} \left[\lambda_{i,t}^8\right] \tag{26}$$

$$|V_i|^{\min} \le \left|V_{i,t}\right| \le |V_i|^{\max},$$
$$\forall i \in \Omega_N, t \in \mathcal{T} \left[\lambda_{i,t}^9, \lambda_{i,t}^{10}\right] \tag{27}$$

$$\left. 0 \le \rho_{i,t} \le 1, \ \forall i \in \Omega_N, t \in \mathcal{T} \quad \left[\lambda_{i,t}^{11}\right] \right\} \tag{28}$$

The objective function (9) is to minimize the hardening investment and the projected load shedding cost under the worst scenarios. The hardening investment and load shedding cost are represented by (10) and (11), respectively. The first-level problem consists equation (9) and constraints (12)-(13). Constraint (12) limits the hardening investment budget. Constraint (13) indicates that only one hardening strategy can be selected for each line.

In the second level, the damage caused by failures of hardened lines during extreme weather events is maximized, which can be modeled by the second part of the objective function (9) and constraints (14)-(18).

Constraints (14)-(16) generate the damage uncertainty set of distribution systems at time t. Constraint (14) provides the system uncertainty budget. The definition of this constraint is related to the Claude Shannon's information theory [16]. $\mathcal{W}$ represents the uncertainty budget which can be decided by system planners. In particular, a line with a lower failure probability takes up more uncertainty budget if it fails and vice versa. For example, if the failure probability of a line is zero, then it takes an infinite uncertainty budget and $z_{ij,t}^k = 0$. If the failure probability is one, then it takes zero budget and $z_{ij,t}^k = 1$. Therefore, a smaller $\mathcal{W}$ represents a larger upper limit of the number of failed lines. In (14), $p_{ij,t}^k$ represents the failure probability of line ij before being damaged by extreme weather events, if it is hardened by the k-th strategy ($k = 1, \ldots, 4$). For example, if $k = 1$, $p_{ij,t}^1$ is the failure probability of line ij after being hardened by pole upgrading. If $k = 2$, $p_{ij,t}^2$ is the failure probability of line ij after being hardened by tree trimming. If $k = 3$, $p_{ij,t}^3$ is the failure probability of line ij after being hardened by the combination strategy of upgrading pole and tree trimming. If $k = 4$, $p_{ij,t}^4$ is the failure probability of line ij without implementing any hardening strategy. $p_{ij,t}^k$ can be calculated using equations (1)-(8) with the parameters of different hardening strategies. Constraint (15) indicates that

the failure of line *ij* after being hardened by a specific strategy can only occur when that strategy is selected in the first level. Constraint (16) assumes that the failure of line *ij* after being hardened by a specific strategy only occurs once during the 24 hours of the extreme weather event. Constraint (17) imposes the repair time of the damaged line *ij*, where T_R is assumed to be the repair time. If a line starts to be out of service at time *st*, it remains failed until being repaired. For example, if $T_R = 18$ and $z^k_{ij,4} = 1$, $u_{ij,t} \le 1, t = 4, \ldots, 22$.

The third level is to minimize the cost of load shedding due to out-of-service lines. Constraints (19) and (20) represent the power balance at each node. Constraints (21) and (22) enforce the line flow limits and represent the network connectivity. If line *ij* is damaged, $u_{ij,t} = 1$, then $P_{ij,t} = 0$ and $Q_{ij,t} = 0$. Constraints (23) and (24) represent the voltage level at each node. Constraints (19)-(20) and (23)-(24) are linearized DistFlow equations which have been widely used to calculate the complex power flow and voltage profile in problems such as DG placement, service restoration, system operation, and planning of distribution systems [17]–[20]. Constraints (25) and (26) limit active and reactive power output of DGs, respectively. Constraint (27) imposes the voltage limits. Constraint (28) imposes an upper bound on load shedding ratios.

In the above formulation, x^k_{ij} represents the first-level decision variables; $z^k_{ij,t}$, $u_{ij,t}$ are the second-level decision variables, and the third-level decision variables are $P^g_{i,t}$, $P_{ij,t}$, $Q_{ij,t}$, and $|V_{i,t}|$. The variables in the brackets following constraints (19)-(28) represent dual variables of these constraints. Constraint (27) has two dual variables to represent the inequalities.

IV. Solution Algorithm

In this tri-level model, some variables in the first and second levels are coupled, i.e., x^k_{ij}, $z^k_{ij,t}$, and $u_{ij,t}$. The out-of-service distribution lines are determined by the severity of extreme weather events and the selected hardening strategies. As a result, it cannot be directly decoupled into a sub-problem and a master problem as proposed in [21]. To solve this challenge, a greedy search methodology is proposed. The tri-level model is reformulated as a bi-level problem. The upper level is to select optimal hardening strategies for critical lines. The lower level is to identify critical lines which are the most vulnerable to extreme weather events and have severe impacts on load shedding. The *max-min* structure in the second and third level of the tri-level model is reformulated into a single-level equivalent.

A. Problem Reformulation

One popular method to solve the *max-min* problem is to reformulate it into a single-level problem using the Karush-Kuhn-Tucker (KKT) conditions, and then linearize the complementarity constraints with the big-*M* method [21]. In this paper, we firstly dualize the *max-min* problem by introducing bilinear terms, and then linearize these terms by exploiting the discrete structure of the uncertainty set. The lower level identifies the worst-case scenario given a hardening decision *x*. It is denoted as $\mathcal{R}(x)$ and can be formulated as:

$$\max_{u\in\mathcal{U}} \min_{o\in\mathcal{O}(u)} C^S(o) \tag{29}$$

The Lagrangian equation is:

$$\begin{aligned}
\mathcal{L} = & \sum_{i\in\Omega_L}\sum_{t\in\mathcal{T}} c^L_i \rho_{i,t} P^L_{i,t} \\
& + \sum_{t\in\mathcal{T}} \lambda^1_{i,t}\left[\sum_{\{j|(i,j)\in\Omega_B\}} P_{ij,t} - P^g_{i,t} - \sum_{\{j|(i,j)\in\Omega_B\}} P_{ji,t} + \big(1-\rho_{i,t}\big)P^L_{i,t}\right] \\
& + \sum_{t\in\mathcal{T}} \lambda^2_{ij,t}\left[\sum_{\{j|(i,j)\in\Omega_B\}} Q_{ij,t} - \sum_{\{j|(i,j)\in\Omega_B\}} Q_{ji,t} - Q^g_{i,t} + \big(1-\rho_{i,t}\big)Q^L_{i,t}\right] \\
& + \sum_{t\in\mathcal{T}}\sum_{(i,j)\in\Omega_B} \lambda^3_{ij,t}\Big[P_{ij,t} - \big(1-u_{ij,t}\big)P^{\max}_{ij}\Big] \\
& + \sum_{t\in\mathcal{T}}\sum_{(i,j)\in\Omega_B} \lambda^4_{ij,t}\Big[Q_{ij,t} - \big(1-u_{ij,t}\big)Q^{\max}_{ij}\Big] \\
& + \sum_{t\in\mathcal{T}}\sum_{j\in\Omega_N} \lambda^5_{i,t}\Big(\big|V_{j,t}\big| - \big|V_{i,t}\big| + \frac{R_{ij}P_{ij,t} + X_{ij}Q_{ij,t}}{V_0} \\
& \qquad - u_{ij,t}M_1\Big) \\
& + \sum_{t\in\mathcal{T}}\sum_{j\in\Omega_N} \lambda^6_{i,t}\Big(-\big|V_{j,t}\big| + \big|V_{i,t}\big| - u_{ij,t}M_1 \\
& \qquad - \frac{R_{ij}P_{ij,t} + X_{ij}Q_{ij,t}}{V_0}\Big) \\
& + \sum_{t\in\mathcal{T}}\sum_{i\in\Omega_G} \lambda^7_{i,t}\big(P^g_{i,t} - P^{g,\max}_{i,t}\big) \\
& + \sum_{t\in\mathcal{T}}\sum_{i\in\Omega_G} \lambda^8_{i,t}\big(Q^g_{i,t} - Q^{g,\max}_{i,t}\big) \\
& + \sum_{t\in\mathcal{T}}\sum_{i\in\Omega_N} \lambda^9_{i,t}\Big(-\big|V_{i,t}\big| + \big|V_{i,t}\big|^{\min}\Big) \\
& + \sum_{t\in\mathcal{T}}\sum_{i\in\Omega_N} \lambda^{10}_{i,t}\big(\big|V_{i,t}\big| - \big|V_{i,t}\big|^{\max}\big) + \sum_{t\in\mathcal{T}}\sum_{i\in\Omega_N} \lambda^{11}_{i,t}\big(\rho_{i,t} - 1\big)
\end{aligned} \tag{30}$$

whose optimality occurs at

$$\frac{\partial\mathcal{L}}{\partial P_{ij,t}} = \lambda^1_{i,t} - \lambda^1_{j,t} + \lambda^3_{ij,t} + \frac{R_{ij}}{V_0}\lambda^5_{ij,t} - \frac{R_{ij}}{V_0}\lambda^6_{ij,t} = 0 \tag{31}$$

$$\frac{\partial\mathcal{L}}{\partial Q_{ij,t}} = \lambda^2_{i,t} - \lambda^2_{j,t} + \lambda^4_{ij,t} + \frac{X_{ij}}{V_0}\lambda^5_{ij,t} - \frac{X_{ij}}{V_0}\lambda^6_{ij,t} = 0 \tag{32}$$

$$\frac{\partial\mathcal{L}}{\partial V_{i,t}} = -\sum_{j\in\Omega_N}\lambda^5_{ij,t} + \sum_{j\in\Omega_N}\lambda^5_{ji,t} - \lambda^9_{i,t} + \lambda^{10}_{i,t} = 0 \tag{33}$$

$$\frac{\partial\mathcal{L}}{\partial P^g_{i,t}} = -\lambda^1_{i,t} + \lambda^7_{i,t} \ge 0 \tag{34}$$

$$\frac{\partial\mathcal{L}}{\partial Q^g_{i,t}} = -\lambda^2_{i,t} + \lambda^8_{i,t} \ge 0 \tag{35}$$

$$\frac{\partial\mathcal{L}}{\partial \rho_{i,t}} = c^L_i P^L_{i,t} - \lambda^1_{i,t}P^L_{i,t} + \lambda^{11}_{i,t} - \lambda^2_{i,t}Q^L_{i,t} \ge 0 \tag{36}$$

By using the optimality condition, we can reformulate $\mathcal{R}(x)$ as follows.

$$\begin{aligned} Max \ & \sum_{t\in\mathcal{T}}\sum_{i\in\Omega_L} P^L_{i,t}\lambda^1_{i,t} + \sum_{t\in\mathcal{T}}\sum_{i\in\Omega_L} Q^L_{i,t}\lambda^2_{i,t} \\ & - \sum_{t\in\mathcal{T}}\sum_{(i,j)\in\Omega_B} \lambda^3_{ij,t}(1-u_{ij,t})P^{\max}_{ij} \\ & - \sum_{t\in\mathcal{T}}\sum_{(i,j)\in\Omega_B} \lambda^4_{ij,t}(1-u_{ij,t})Q^{\max}_{ij} \\ & - \sum_{t\in\mathcal{T}}\sum_{j\in\Omega_N} \lambda^5_{i,t}u_{ij,t}M_1 - \sum_{t\in\mathcal{T}}\sum_{j\in\Omega_N} \lambda^6_{i,t}u_{ij,t}M_1 \\ & - \sum_{t\in\mathcal{T}}\sum_{i\in\Omega_G} P^{g,\max}_{i,t}\lambda^7_{i,t} - \sum_{t\in\mathcal{T}}\sum_{i\in\Omega_G} Q^{g,\max}_{i,t}\lambda^8_{i,t} \\ & + \sum_{t\in\mathcal{T}}\sum_{i\in\Omega_N} \left|V_{i,t}\right|^{\min}\lambda^9_{i,t} - \sum_{t\in\mathcal{T}}\sum_{i\in\Omega_N} \left|V_{i,t}\right|^{\max}\lambda^{10}_{i,t} \\ & - \sum_{t\in\mathcal{T}}\sum_{i\in\Omega_N} \lambda^{11}_{i,t} \qquad (37) \end{aligned}$$

$$s.t. \ \ u \in \mathcal{U} \qquad (38)$$

$$(31)\text{-}(36)$$

$$\lambda^1_{i,t}, \lambda^2_{ij,t}, free, \forall i \in \Omega_N, (i,j) \in \Omega_B, t \in \mathcal{T} \qquad (39)$$

$$\lambda^3_{ij,t}, \lambda^4_{ij,t}, \lambda^5_{i,t}, \lambda^6_{i,t}, \lambda^7_{ij,t}, \lambda^8_{i,t}, \lambda^9_{i,t}, \lambda^{10}_{i,t}, \lambda^{11}_{i,t} \geq 0, \quad \forall (i,j) \in \Omega_B, i \in \Omega_N, t \in \mathcal{T} \qquad (40)$$

There are bi-linear terms in the objective function (37), e.g., $\lambda^3_{ij,t}(1-u_{ij,t})$ and $\lambda^5_{i,t}u_{ij,t}M_1$. We replace $\lambda^3_{ij,t}(1-u_{ij,t})$ with $\gamma^1_{ij,t}$ and introduce the following two additional constraints.

$$\gamma^1_{ij,t} \geq \lambda^3_{ij,t} - M_2 u_{ij,t} \qquad (41)$$

$$\gamma^1_{ij,t} \geq 0 \qquad (42)$$

where M_2 is a big number. Similarly, the bilinear term $\lambda^4_{ij,t}(1-u_{ij,t})$ is replaced with $\gamma^2_{ij,t}$.

We replace $\lambda^5_{i,t}u_{ij,t}M_1$ with $\gamma^3_{i,t}$ and introduce two additional constrains.

$$\gamma^3_{i,t} \geq \lambda^5_{i,t}M_1 - M_2\left(1-u_{ij,t}\right) \qquad (43)$$

$$\gamma^3_{i,t} \geq 0 \qquad (44)$$

Similarly, the bilinear term $\lambda^4_{i,t}u_{ij,t}M_1$ is replaced with $\gamma^4_{i,t}$.

The optimal hardening strategy selection problem can be denoted as $\mathcal{H}(x)$.

$$\min_x \ \mathcal{C}^I(x) \qquad (45)$$

$$s.t. \ \ x \in \Omega_x \qquad (46)$$

$$\text{Constraint (12)}$$

$$\sum_{(i,j)\in\Omega_B}\left(-\log_2 p^k_{ij,t}\right)z^k_{ij,t} \geq \mathcal{W}, \forall k \in \Omega_x, t \in \mathcal{T} \qquad (47)$$

The objective of (45) is to minimize the hardening investment after the lower level identifies the critical lines. Constraint (46) indicates that for each critical line, only one hardening strategy can be selected. Constraint (47) indicates that the failure probability of hardened critical lines should be lower than a certain limit.

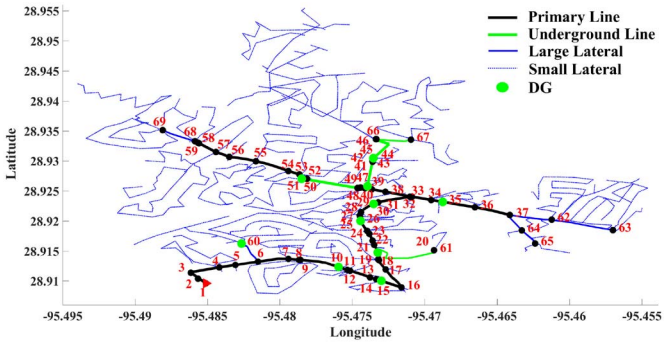

Fig. 2. The modified test system.

Algorithm 1 Greedy Searching Algorithm

Step 0: Initialization. Set the worst extreme weather condition parameters and $s = 0$. Calculate each line's failure probability before hardening.
Step 1: Solve $\mathcal{R}(x^0)$ without any hardening strategy and let (ρ^0, u^0, z^0) denote its optimal solution.
Step 2: Obtain critical lines whose failures have severe impacts on load shedding according **Step 1**'s solution.
Step 3: Update $s \leftarrow s+1$. Calculate failure probabilities of critical lines being hardened by different strategies. Solve $\mathcal{H}(x^s)$, and select the most critical line from Γ^s to be hardened. Use the hardening strategy with the minimum cost to harden that line.
Step 4: Solve $\mathcal{R}(x^s)$ and let (ρ^s, u^s, z^s) denote the optimal solution. Update critical lines in Γ^s.
Step 5: If the investment budget reaches the limit, the algorithm ends; otherwise go to **Step 3**.

B. Solution Algorithm

To solve the problem, we propose a greedy searching algorithm. The algorithm iteratively generates new critical lines in a subset Γ and chooses the most critical line in Γ to be hardened with the minimum cost in each iteration. This means Γ updates the critical lines in every iteration. Note that after one line is selected to be hardened in a certain iteration, the elements in Γ should be changed since the fragility of the entire system changes. $\mathcal{H}(x)$ is solved in each iteration to select a specific critical line in Γ to be hardened by a certain strategy. Given the hardening strategies, $\mathcal{R}(x)$ is solved to update the worst-case scenario to be included in Γ. The algorithm terminates after the investment budget is used up.

V. Numerical Results

In this section, we use a modified Electric Power Research Institute (EPRI) test circuit [22] for case studies. For illustration, the test system is fitted into an area that covers the range of latitude ($28.98°N - 29.05°N$) and longitude ($95.48°W - 95.43°W$), which is close to the coastline, as shown in Fig. 2. This system has a 74-mile primary circuit that supplies 3885 customers, whose voltage level is at $34.5kV$. In Fig. 2, there are 68 lines and 69 nodes in the primary network. The thickness of a line is proportional to the power flowing through the line. A modern power distribution system may have DGs and backup generators, which impacts the system's resilience. To consider these effects, we assume DGs are integrated at nodes 10, 15, 20, 25, 30, 35, 40, 45, 50, and 60,

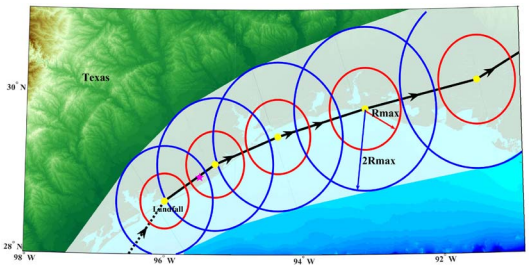

Fig. 3. Category-4 hurricane path tracking.

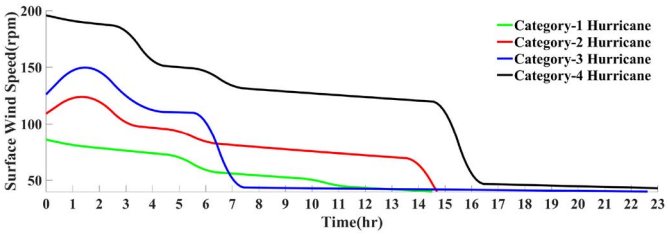

Fig. 4. The surface wind speed variations of hurricanes.

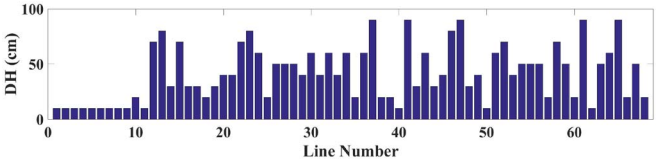

Fig. 5. D_H values of acer rubrum along distribution lines.

TABLE II
THE POLE DATA OF DISTRIBUTION LINES

Pole Type	$\ln(m_R)$	ζ_R	Distribution Line
NESC Class 2	5.05	0.135	L1-2, L2-3, L3-4, L4-5, L5-6, L6-7, L7-8, L8-9, L10-11
NESC Class 3	4.94	0.140	L11-12,L12-13,L13-14,L14-15,L15-16, L16-17,L17-18, L18-19,L19-20,L20-21, L21-22,L22-23,L23-24, L24-25, L25-26, L27-28,L28-29, L29-30,L30-31,L31-32, L32-33,L33-34, L34-35,L35-36,L36-37, L37-38, L39-40,L43-44, L44-45, L50-51, L46-66
NESC Class 5	4.76	0.137	L39-47,L47-48,L48-49,L54-55, L55-56, L56-57,L57-58,L58-59, L6-60,L37-62, L62-63,L58-68, L68-69

each with a capacity of 0.5MW. It is assumed that all DGs are diesel generators used in extreme weather events. DGs at nodes 45 and 50 can provide enough power supply for customers if a flood hits underground lines: L49-50 and L40-41. For demonstration, we consider moderate-to-extreme winds and surge-induced floods in hurricanes as the studied extreme weather events. In order to assess the hurricane's impacts on the distribution system, the hurricane is modeled through its static and dynamic gradient wind fields based on a statistical modeling method [14]. This modeling method provides the spatial spread and intensity of the simulated hurricane, which includes the latitudes and longitudes of the hurricane eye locations, radius to the maximum wind speed of the hurricane, and the wind field.

Based on the above information and the geographic data of the test system, the failure probability of distribution lines can be calculated using (1)-(8). The proposed greedy algorithm can then be used to solve the hardening problem. The subproblem $R()$ is a mixed integer linear programming problem. It is implemented in the GAMS version 24.5.3, and solved using the IBM's CPLEX 12.6 mixed-integer solver. The upper level problem $H()$ is implemented in the Matlab version R2015b. All tests are performed on a PC with 3.6-GHz CPU and 16GB RAM. The computation time is around $20 \sim 30$ minutes which is a reasonable range for planning problems. The voltage range is set as $0.95p.u \sim 1.05p.u$. The uncertainty budget $\mathcal{W}$ is set as 0.2.

A. Hurricane Simulation

For illustration, it is assumed that hurricanes land at the location with latitude $28.6°N$ and longitude $96°W$. The hurricanes are assumed to be moving with a translational speed of 12.5 mph and traveling for 24 hours after landfall [23]. Hence, simulations are performed for a period of 24 hours. In this paper, we consider four categories of hurricanes, i.e., category $1-4$. Fig. 3 illustrates the forecasted track of a category-4 hurricane (with the maximum wind speed at the landfall location), and its time-varying impacts on the test system. The yellow dots represent the locations of the hurricane eye at different times. The magenta star shows the location of the test system. The red circle indicates the boundary of the maximum winds for the traveling hurricanes at a certain eye location. The area between the red circle and the blue circle experiences 82.5% of the maximum wind speed. The wind speed within areas between $2R_{max}$ and $4R_{max}$ is reduced by 25%. As the service area of the test system is relatively small compared to the size of the hurricane, it is assumed that the maximum wind speed at the central point of the test system is applied to all distribution lines [2]. Fig. 4 shows the surface wind speed variations in the middle of the test system as hurricanes of four categories travel along their tracks.

B. System Test Data and Hardening Cost

Table II shows parameters of primary overhead lines in the test system. There are three types of distribution poles in the system, i.e., National Electrical Safety Code (NESC) class 2, class 3 and class 5. Table III shows the data of underground cables. It is assumed that most trees covered in this system are the acer rubrum, and $a_s = -2.261$, $b_s = 0.426$, and $c_s = 0.426$ [13]. Fig. 5 shows the D_H values of acer rubrum along distribution lines. According to the data in Table II, Table III and Fig. 5, the failure probability of distribution lines after being hardened can be calculated using (1)-(8). As shown in Table I, the hardening cost of one line depends on its length.

C. Case1: Without Hardening

It is assumed that the repair time of each failed line is 24 hours. The initial load demand and priority is shown in Fig. 6.

TABLE III
UNDERGROUND LINE DATA

Underground Cable	Category of surge zone	Length (ft)	a	b
L40-41	2	1648	0.03	0.06
L42-43	2	176	0.0033	0.06
L45-46	2	2083	0.039	0.06
L49-50	2	1572	0.03	0.06
L51-52	5	107.5	0.002	0.06
L20-61	5	2559.8	0.048	0.06
L66-67	5	1664.2	0.031	0.06

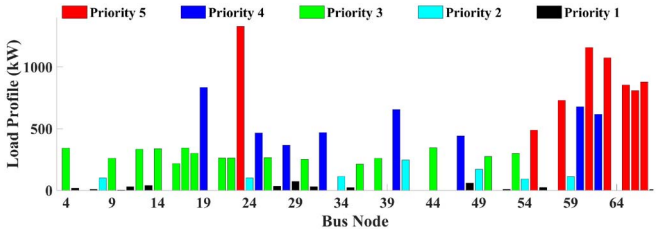

Fig. 6. The load demand at $t = 0$.

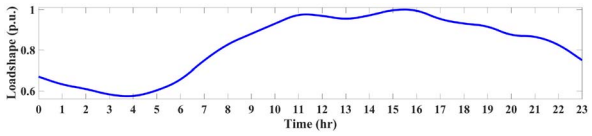

Fig. 7. The loadshape for 24 hours.

The total load demand at $t = 0$ is $30.43MW$. The load priorities are divided into 5 categories with priority 5 as the highest one. The 24-hour load shape is shown in Fig. 7. The basic load shedding cost is assumed to be $\$14/kWh$ [24] and the load shedding cost parameter c_i^L in equation (11) is the product of the basic load shedding cost and the load priority. We consider the worst-case scenario, i.e., the category-4 hurricane. If there is no grid hardening, the failed lines are L15-16, L6-60, L24-25, L36-37, L37-62, L39-47, L47-48, L48-49, L52-53, L53-54, L54-55, L55-56, L56-57, L57-58, and L58-59, as shown in Fig. 8 (a). In this figure, red dotted lines represent damaged distribution lines and green dots represent existing DGs. This worst-case scenario results in $615.34MWh$ load shedding in the 24-hour repair period. The total load shedding cost is \$51,832,148.26.

D. Case2: With Hardening

In this case, we consider hardening the system to protect against extreme winds and floods induced by category-4 hurricanes. The hardening budget is assumed to be \$237,000. By using the model and solution algorithm proposed in Section IV, the optimal hardening plan and load shedding cost are calculated and shown in Table IV. In each iteration, one line is selected to be hardened and the number of failed lines are updated. For example, if one critical line (L24-25) is hardened by upgrading poles, the load shedding cost decreases to \$46,872,116.25, which is a reduction of 9.57%. In the fourth iteration, there are still 15 lines failed but the total load shedding cost has decreased to \$30,945,260.46, which is a reduction of 40.30%. When the budget is used up, the load shedding cost is reduced by more than 84% compared to case 1. The total hardening investment cost after hardening L48-49 is \$236,595. If the algorithm continues to harden lines, the investment cost will reach \$284,534, which exceeds the investment budget. As a result, the algorithm ends after hardening L48-49.

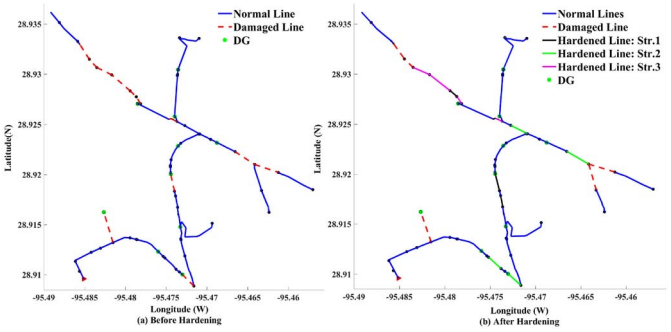

Fig. 8. The distribution network before and after hardening.

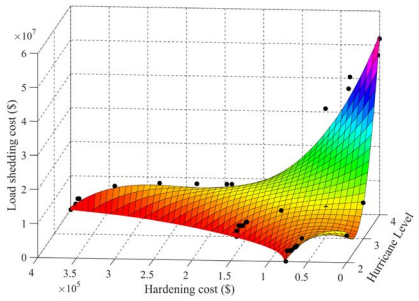

Fig. 9. Load shedding costs under different hardening investments and hurricane levels.

Furthermore, the hardening strategy for each line depends on its hardening cost and line conditions such as original pole classes. Fig. 8 shows the comparison of damaged lines before and after hardening. There are 16 damaged lines in Fig. 8 (a), and the number of damaged lines in Fig. 8 (b) has decreased to 8. Fig. 8 (b) also shows the locations and hardening strategies of distribution lines. Blue lines indicate that no hardening strategy is selected for the line, black lines are hardened by upgrading poles, green lines are hardened by trimming trees, and magenta lines are hardened by Strategy 3.

E. Case3: Sensitivity Analysis

To show the impacts of investment budgets and hurricane severities on system resilience, we perform a sensitivity analysis of load shedding costs with different hardening investments and hurricane levels. The results are shown in Fig. 9. Since the category-1 hurricane does not have impacts on distribution systems, this figure illustrates the worst-case scenarios of category-2, category-3, and category-4 hurricanes. Fig. 9 indicates that for all worst-case hurricanes, the load shedding costs are proportionally decreasing with respect to the increasing of hardening budgets. Meanwhile, a more severe hurricane results

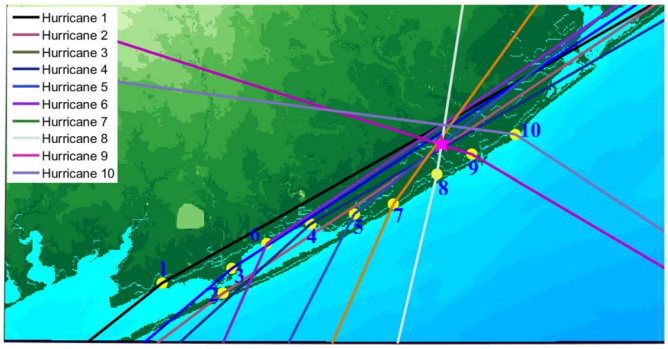

Fig. 10. Traveling paths of different hurricanes with different landfall points.

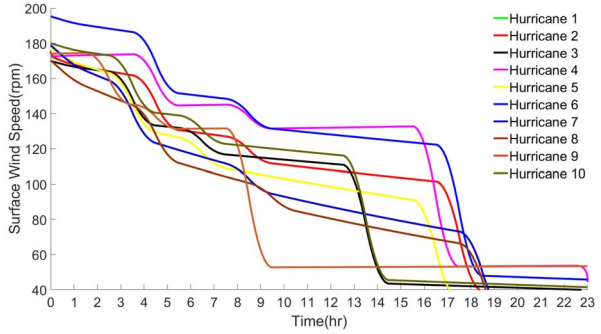

Fig. 11. The surface wind speed variations of 10 different hurricanes.

TABLE IV
OPTIMAL HARDENING PLANS FOR CATEGORY-4 HURRICANE

No	Hardened Line	Strategy	Hardening Cost ($)	Load Shedding Cost ($)	Total Failed Lines
1	L24-25	1	2,437.13	46,872,116.24	16
2	L33-38	2	3,5954.20	40,367,134.84	15
3	L22-23	1	1,589.79	36,937,089.47	15
4	L15-16	2	29,961.83	30,945,260.46	14
5	L12-13	2	29,961.83	13,819,127.47	15
6	L46-66	3	5,992.37	10,435,943.94	15
7	L39-47	3	12,695.40	9,709,752.35	14
8	L52-53	3	19,389.63	9,341,072.20	13
9	L53-54	1	1337.81	9,267,009.32	12
10	L54-55	3	51,787.92	8,264,433.90	11
11	L47-48	3	6,437.88	8,241,964.90	10
12	L55-56	3	38,714.86	8,233,018.56	9
13	L48-49	1	334.43	8,233,018.56	8

in higher load shedding costs and requires larger hardening investments.

F. Case4: Multi-Landfall Points

In the above simulations, there is a single landfall point for hurricanes. In this case, we consider multiple entry points of different category-4 hurricanes, and find the worst case of each landfall point. As the traveling direction of most hurricanes in Texas since 1960 is from southwest to northwest, we consider 10 landfall points around the test system in this case study. Fig. 10 shows different landfall points with different traveling paths of hurricanes. Fig. 11 shows the surface wind speed variations in the middle of the test system under 10 category-4 hurricanes. It is assumed that the hardening investment budget is still $237,000. The hardening results are shown in Table V.

TABLE V
OPTIMAL HARDENING PLANS FOR MULTIPLE ENTRIES OF HURRICANES

Scenario	Hardened Lines	Investment Cost ($)	Load Shedding Cost ($)
1	L24-25, L46-66, L33-38, L22-23, L15-16, L12-13, L39-47, L52-53, L53-54, L54-55, L47-48, L55-56 L48-49	236,595	8,232,659.72
2	L24-25, L33-38, L22-23, L15-16, L12-13, L46-66, L39-47, L52-53, L53-54, L54-55, L47-48, L55-56 L48-49	236,595	8,232,659.72
3	L24-25, L33-38, L22-23, L15-16, L12-13, L46-66, L39-47, L52-53, L53-54, L54-55, L47-48, L55-56 L48-49	236,595	8,232,659.72
4	L22-23, L15-16, L46-66, L12-13, L52-53, L39-47, L33-38, L53-54, L54-55, L47-48, L55-56, L48-49 L24-25	236,595	8,232,659.72
5	L46-66, L22-23, L24-25, L23-24, L15-16, L12-13, L13-14, L52-53, L39-47, L33-38,L53-54, L54-55, L47-48	209,530	8,241,964.90
6	L46-66, L22-23, L24-25, L23-24, L15-16, L12-13, L13-14, L52-53, L39-47, L33-38,L53-54, L54-55, L47-48	209,530	8,241,964.90
7	L46-66, L22-23, L23-24, L24-25, L15-16, L33-38, L12-13, L13-14, L39-47, L52-53, L31-32, L53-54 L54-55, L47-48	212,833	8,241,964,90
8	L24-25, L33-38, L22-23, L15-16, L12-13, L46-66, L39-47, L52-53, L53-54, L54-55, L47-48, L55-56 L48-49	236,595	8,232,659.72
9	L22-23, L15-16, L46-66, L12-13, L52-53, L39-47, L33-38, L53-54, L54-55, L47-48, L55-56, L48-49 L24-25	236,595	8,232,659.72
10	L46-66, L22-23, L15-16, L12-13, L13-14, L52-53, L39-47, L33-38, L23-24, L53-54, L54-55, L31-32 L24-25, L47-48	212,833	8,241,964.90

We can see from this table that the hardening plans under 6 worst-case scenarios (Scenario 1, 2, 3, 4, 8, and 9) are the same as the hardening decisions in Table IV. The hardening plans under scenario 5, 6, 7, 10 are a little different from Table IV (most hardened lines are the same, only two lines are different). These results indicate that the landfall positions of hurricanes do not severely affect the uncertain set of the hardening problem.

VI. Conclusion

This paper presents a new approach for hardening distribution systems to protect against extreme weather events. The problem is formulated as a tri-level mixed-integer linear program, and then reformulated as a bi-level problem. The first level solves the hardening investment problem, and the second level models system operations under the worst-case scenarios. The proposed model is tested on a modified EPRI test circuit. Numerical results show that the proposed model can assist utilities to identify optimal hardening strategies to mitigate systems' vulnerability to extreme weather. Compared to previous efforts on power system hardening, the proposed method is more practical since it considers the severities of extreme weather events, the worst-case scenarios and the probabilistic failures of hardened components.

References

[1] D. T. Ton and W.-T. P. Wang, "A more resilient grid: The U.S. department of energy joins with stakeholders in an R&D plan," *IEEE Power Energy Mag.*, vol. 13, no. 3, pp. 26–34, May/Jun. 2015.

[2] A. M. Salman, Y. Li, and M. G. Stewart, "Evaluating system reliability and targeted hardening strategies of power distribution systems subjected to hurricanes," *Rel. Eng. Syst. Safety*, vol. 144, pp. 319–333, Dec. 2015.

[3] E. Yamangil, R. Bent, and S. Backhaus, "Resilient upgrade of electrical distribution grids," in *Proc. 29th AAAI Conf.*, Austin, TX, USA, Jan. 2015, pp. 1233–1240.

[4] Executive Office of the President, *Economic Benefits of Increasing Electric Grid Resilience to Weather Outages*, IEEE USA Books & eBooks, Washington, DC, USA, Aug. 2013, p. 29. [Online]. Available: http://energy.gov/sites/prod/files/2013/08/f2/Grid%20Resiliency%20Report_FINAL.pdf

[5] G. Li *et al.*, "Risk analysis for distribution systems in the Northeast U.S. under wind storms," *IEEE Trans. Power Syst.*, vol. 29, no. 2, pp. 889–898, Mar. 2014.

[6] R. E. Brown, "Hurricane hardening efforts in Florida," in *Proc. IEEE Power Energy Soc. Gen. Meeting*, Pittsburgh, PA, USA, Jul. 2008, pp. 1–7.

[7] P. A. Kuntz, R. D. Christie, and S. S. Venkata, "Optimal vegetation maintenance scheduling of overhead electric power distribution systems," *IEEE Trans. Power Del.*, vol. 17, no. 4, pp. 1164–1169, Oct. 2002.

[8] N. Alguacil, A. Delgadillo, and J. M. Arroyo, "A trilevel programming approach for electric grid defense planning," *Comput. Oper. Res.*, vol. 41, no. 1, pp. 282–290, Jan. 2014.

[9] W. Yuan, L. Zhao, and B. Zeng, "Optimal power grid protection through a defender-attacker-defender model," *Rel. Eng. Syst. Safety*, vol. 121, pp. 83–89, Jan. 2014.

[10] A. Gholami, F. Aminifar, and M. Shahidehpour, "Front lines against the darkness: Enhancing the resilience of the electricity grid through microgrid facilities," *IEEE Electrification Mag.*, vol. 4, no. 1, pp. 18–24, Mar. 2016.

[11] R. Brown, "Cost-benefit analysis of the deployment of utility infrastructure upgrades and storm hardening programs," Quanta Technol., Raleigh, NC, USA, Tech. Rep. 36375, Mar. 2009. [Online]. Available: http://www.puc.texas.gov/industry/electric/reports/infra/utlity_infrastructure_upgrades_rpt.pdf

[12] M. Ouyang and L. Dueñas-Osorio, "Multi-dimensional hurricane resilience assessment of electric power systems," *Struct. Safety*, vol. 48, pp. 15–24, May 2014.

[13] C. D. Canham, M. J. Papaik, and E. F. Latty, "Interspecific variation in susceptibility to windthrow as a function of tree size and storm severity for northern temperate tree species," *Can. J. Forest Res.*, vol. 31, no. 1, pp. 1–10, Jan. 2001.

[14] L. Xu, "Underground assessment phase 3 report: Ex ante cost and benefit modeling," Quanta Technol., Raleigh, NC, USA, Tech. Rep. PSC-06-035-PAA-EI, May 2008. [Online]. Available: http://www.feca.com/PURCPhase3FinalReport.pdf

[15] D. Louth. (Dec. 2011). *Governor's Two-Storm Panel: Distribution Infrastructure Hardening Options and Recommendations*. [Online]. Available: http://www.ctconstruction.org/files/public/Two_Storm_Panel_Storm_Hardening.pdf

[16] *7th AIMMS/MOPTA Optimization Modeling Competition*. Accessed on Jul. 20, 2015. [Online]. Available: http://coral.ie.lehigh.edu/~mopta2015/AIMMS_MOPTA_case_2015.pdf

[17] M. E. Baran and F. F. Wu, "Network reconfiguration in distribution systems for loss reduction and load balancing," *IEEE Trans. Power Del.*, vol. 4, no. 2, pp. 1401–1407, Apr. 1989.

[18] Z. Wang, B. Chen, J. Wang, J. Kim, and M. Begovic, "Robust optimization based optimal DG placement in microgrids," *IEEE Trans. Smart Grid*, vol. 5, no. 5, pp. 2173–2182, Sep. 2014.

[19] C. Chen, J. Wang, F. Qiu, and D. Zhao, "Resilient distribution system by microgrids formation after natural disasters," *IEEE Trans. Smart Grid*, vol. 7, no. 2, pp. 958–966, Mar. 2016.

[20] Z. Wang, B. Chen, J. Wang, and C. Chen, "Networked microgrids for self-healing power systems," *IEEE Trans. Smart Grid*, vol. 7, no. 1, pp. 310–319, Jan. 2016.

[21] B. Chen, J. Wang, L. Wang, Y. He, and Z. Wang, "Robust optimization for transmission expansion planning: Minimax cost vs. minimax regret," *IEEE Trans. Power Syst.*, vol. 29, no. 6, pp. 3069–3077, Nov. 2014.

[22] *Summary of EPRI Test Circuits*, EPRI, Palo Alto, CA, USA, 2012, pp. 1–4.

[23] *Forward Speed of a Hurricane, Hurricane Research Division*. Accessed on May 29, 2014. [Online]. Available: http://www.aoml.noaa.gov/hrd/tcfaq/G16.html

[24] R. E. Brown, *Electric Power Distribution Reliability*. New York, NY, USA: CRC Press, 2008.

Shanshan Ma received the B.S. degree in information and electrical engineering from Zhejiang University City College, Hangzhou, China, in 2012, and the M.S. degree from the Department of Electrical Engineering and Computer Science, South Dakota State University, Brookings, SD, USA, in 2015. She is currently pursuing the Ph.D. degree with the Department of Electrical and Computer Engineering, Iowa State University, Ames, IA, USA. Her current research interests include self-healing resilient distribution systems, and microgrids.

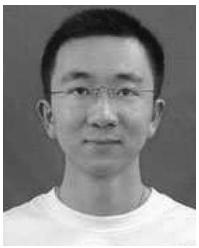

Bokan Chen received the B.S. degree in electronics and information engineering from the Huazhong University of Science and Technology, Wuhan, China, in 2011, and the M.S. degree from the Department of Industrial and Manufacturing System Engineering, Iowa State University, Ames, IA, USA, where he is currently pursuing the Ph.D. degree. His current research interests include optimization theories and their applications.

Zhaoyu Wang received the B.S. and M.S. degrees in electrical engineering from Shanghai Jiao Tong University in 2009 and 2012, respectively, and the M.S. and Ph.D. degrees in electrical and computer engineering from the Georgia Institute of Technology in 2012 and 2015, respectively. He is an Assistant Professor with Iowa State University. He was a Research Aid with Argonne National Laboratory in 2013 and an Electrical Engineer with Corning Inc., in 2014. His research interests include power distribution systems, microgrids, renewable integration, self-healing resilient power systems, and voltage/VAR control.